Research Article

Sajjad Hussain, Muhammad Mubeen*, Ashfaq Ahmad, Nasir Masood*, Hafiz Mohkum Hammad, Muhammad Amjad, Muhammad Imran, Muhammad Usman, Hafiz Umar Farid, Shah Fahad, Wajid Nasim, Hafiz Muhammad Rashad Javeed, Mazhar Ali, Saeed Ahmad Qaisrani, Amjad Farooq, Muhammad Shafique Khalid, and Mirza Waleed

# Satellite-based evaluation of temporal change in cultivated land in Southern Punjab (Multan region) through dynamics of vegetation and land surface temperature

https://doi.org/10.1515/geo-2020-0298
received January 29, 2021; accepted September 13, 2021

**Abstract:** The rapid increase in urbanization has an important effect on cropping pattern and land use/land cover (LULC) through replacing areas of vegetation with commercial and residential coverage, thereby increasing the land surface temperature (LST). The LST information is significant to understand the environmental changes, urban climatology, anthropogenic activities, and ecological interactions, etc. Using remote sensing (RS) data, the present research provides a comprehensive study of LULC and LST changes in water scarce and climate prone Southern Punjab (Multan region), Pakistan, for 30 years (from 1990 to 2020). For this research, Landsat images were processed through supervised classification with maps of the Multan region. The LULC changes showed that sugarcane and rice (decreased by 2.9 and 1.6%, respectively) had less volatility of variation in comparison with both wheat and cotton (decreased by 5.3 and 6.6%, respectively). The analysis of normalized difference vegetation index (NDVI) showed that the vegetation decreased in the region both in minimum value (−0.05 [1990] to −0.15 [2020]) and maximum value (0.6 [1990] to 0.54 [2020]). The results showed that the built-up area was increased 3.5% during 1990–2020, and these were some of the major changes which increased the LST (from 27.6 to 28.5°C) in the study area. The significant regression in our study clearly shows that NDVI and LST are negatively correlated with each other. The results suggested that increasing temperature in growing period had a greatest effect on all types of vegetation. Crop-based classification aids water policy managers and analysts to make a better policy with enhanced information based on the extent of the natural resources. So, the study of dynamics in major crops and surface temperature through satellite RS can play an important role in the rural development and planning for food security in the study area.

**Keywords:** remote sensing, LST, accuracy assessment, crops, geographic information system, normalized difference vegetation index

## 1 Introduction

During the last few years, climate scientists' attention has been progressively drawn to regional as well as local

*** Corresponding author: Muhammad Mubeen,** Department of Environmental Sciences, COMSATS University Islamabad, Vehari Campus, 61100, Vehari, Pakistan,
e-mail: muhammadmubeen@cuivehari.edu.pk
*** Corresponding author: Nasir Masood,** Department of Environmental Sciences, COMSATS University Islamabad, Vehari Campus, 61100, Vehari, Pakistan, e-mail: nasirmasood@ciitvehari.edu.pk
**Sajjad Hussain, Muhammad Amjad, Muhammad Imran, Hafiz Muhammad Rashad Javeed, Mazhar Ali, Saeed Ahmad Qaisrani, Amjad Farooq, Muhammad Shafique Khalid, Mirza Waleed:** Department of Environmental Sciences, COMSATS University Islamabad, Vehari Campus, 61100, Pakistan
**Ashfaq Ahmad:** Asian Disaster Preparedness Center (ADPC), Bangkok, Thailand
**Hafiz Mohkum Hammad:** Department of Agronomy, Muhammad Nawaz Sharif University of Agriculture, Multan 66000, Pakistan
**Muhammad Usman:** Department of Geoecology, Institute of Geosciences and Geography, Room: H4 1.30, Von-Seckendorff-Platz 4, 06120 Halle (Saale), Germany
**Hafiz Umar Farid:** Department of Agricultural Engineering, Bahauddin Zakariya University, Multan, Pakistan
**Shah Fahad:** Department of Agronomy, The University of Haripur, Haripur 22620, Pakistan
**Wajid Nasim:** Department of Agronomy, Faculty of Agriculture and Environment, The Islamia University of Bahawalpur (IUB), Punjab, Pakistan

climates to understand the increasing variation in climate driving factors because of human activities [1–3]. The information about present land use/land cover (LULC) trends is one of the significant need to address the difficulties related with land use management [4–6]. Latest, reliable, and adequate LULC knowledge about the previous to current LULC variations are vital to evaluate and understand different social, economic, and ecological consequences of these variations [7,8]. To assist the LULC classes, expert's knowledge and local information on the growing methods of crops have been used in different studies [9,10], which has helped to determine crop cycles and specific crops [11]. Spatial analysis of rice region at a spatial scale of 5 min arc and mapping of rice in South Asian countries by using Landsat images are the latest additions in previous few years in remote sensing (RS) field [12–14]. Apart from mapping of various cropping patterns, different LULC databases have been established [15]. The LULC classification helps in delineating the cropping pattern of extensive areas, along with understanding the crop rotation and crop intensity in different regions [16].

The land surface temperature (LST) is a main parameter for world's energy budget [17]. Hence, studying changes in LST is essential in providing fundamental information for human survival [18]. Various studies use LST as a suitable parameter in different fields (urban climate, hydrological series, climate change and vegetation monitoring, socioeconomic variables like population density, as well as environmental observations) [19–22]. Correct spatial analysis of LST is becoming more important in providing information about LULC properties [23], and the use of Landsat data has become one of the main resources to observe the LST on regional as well as local scales [24–26]. To analyze and quantify the urban heat island effect, researchers have used satellite images like Landsat 8 Operational Land Imager (OLI) [27,28]. Climatic variations and extreme weather events negatively influenced the crop growth and their development, which may reduce the crop output significantly [29].

Normalized difference vegetation index (NDVI) is used to identify the crop condition, and forecast yield in different countries all over the world [30,31]. The NDVI model was developed based on the principle that greenest vegetation has less reflectance in the visible portion of the electromagnetic spectrum due to chlorophyll and further pigment absorption; however, the vegetation has maximum reflectance in the near-infrared (NIR) because of inside reflectance by the mesophyll spongy tissue of green leaf [32–34]. However, the time-based analysis of complete LULC classes (based on NDVI) is still unmapped but is accomplishable by using Landsat data that provides cost-free information with NDVI after every 16 days at greater spatial resolution [35,36]. This resolution is sufficient in taking practically all main crop classes for accurate measurement of crop water requirements and subsequent water distribution planning for different parts of irrigated areas [37,38].

In the twentieth century, the worldwide temperature was increased by 0.60°C, and the initial few years of twenty-first century was found to be the warmest years of the earth intergovernmental panel on climate change. According to the Global Climate Risk Index (GCRI) 2014, Pakistan ranked third among the badly climate-affected countries. While studying the demographic trend, we see that from 1951 to 1998, the population of Punjab province increased by 258% and from 1998 to 2010 by 26% [40]. Agriculture is the largest and very important sector of Southern Punjab economy, which uses more than 50% of total work force and contributes a vital role in the economic prosperity of the country. Temperature is a dominating factor in arid and semi-arid climatology of southern Punjab (Multan division) [41]. *Rabi* and *Kharif* are the two main cropping seasons, and these seasons are significant to shape the agricultural production in Punjab under different climate scenarios [31]. The Multan division consists of plains with productive land and is a part of Indus plain; it is appropriate for wheat, cotton, rice, sugarcane, rabi and kharif fodder, and many other crops. But during the last few years, various cropped area decreased and converted into urban areas in Southern Punjab [34]. To study past trend is quite important to know the effect of climate change on the agricultural production of the area in future. So, the main objective of this research is to analyze the LULC and LST changes by using Landsat data from 1990 to 2020 through the combination of RS and geographic information system (GIS). The current study aimed to (1) quantify various LULC classes as well as estimate cropping pattern from 1990 to 2020 in Multan region, Pakistan, (2) use the GIS tools for reliable examining of the changes in LST and NDVI, and (3) understand the relationship of climate factor like LST with NDVI in Multan division, Pakistan.

# 2 Methods

## 2.1 Study area and cropping calendar

The study area selected was Multan division located in Southern Punjab (Pakistan). This area lies between

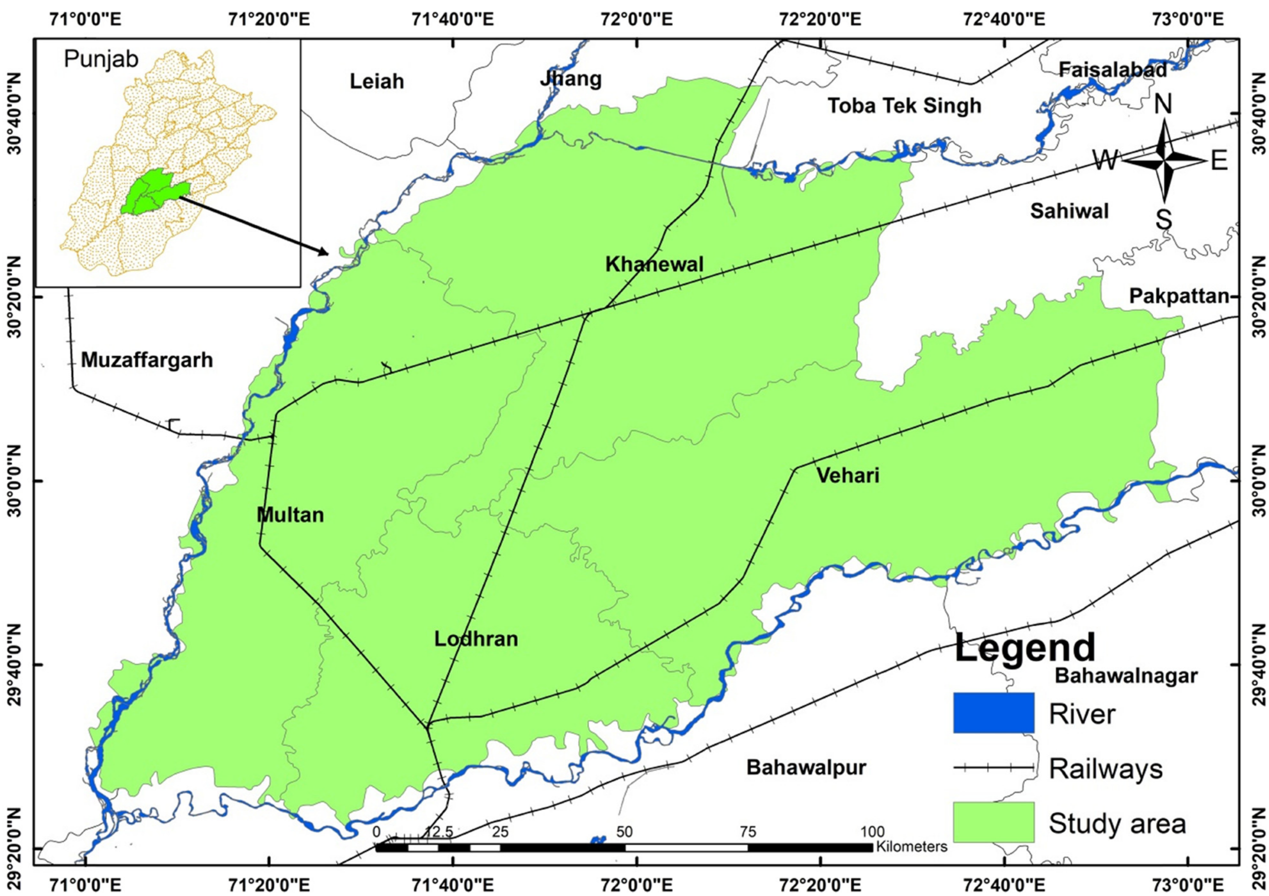


**Figure 1:** Location of the study area (Multan division).

latitude 29° 27′ 21″ N to 30° 45′ 30″ N and longitude 71° 00′ 54″ E to 72° 58′ 43″ E approximately (Figure 1). The Multan division has four districts namely Multan, Khanewal, Lodhran, and Vehari districts. The study area is bounded by districts Jhang and Toba Tek Singh on the north, the districts Bahawalnagar and Bahawalpur on the south, the district Pakpattan on the east, and the district Muzaffargarh on the west. Multan division lies at Nili Bar, which is situated among Ravi, Beas, and Sutlej rivers. Many canals are present here that irrigate Multan region. The area is an alluvial plain and flat, which is an ideal area for agricultural activities. This irrigation network of canals makes the land very fertile. In the monsoon season, land area close to the Chenab river is usually flooded. All area with very hot summers and mild winters features has an arid climate. The average rainfall is roughly 186 mm (7.3 inch). The area witnesses some of the most extreme weathers in the country with highest recorded temperature approximately 52°C (126°F), during 2010 and the lowest recorded temperature approximately −1°C (30°F) [40]. Dust storms are a common phenomenon in the area. Multan region lies in cotton-wheat cropping zone of Punjab. Wheat is the major crop of *Rabi* season, and cotton is the major crop of *Kharif* season in Multan region.

The cropping calendar is a tool, which provides complete data about crop phenology from sowing up to harvest; it contributes to devising the management plans required for sound agronomic practices and yield production assessments, etc. Cropping pattern of Multan division has two growing periods, namely kharif (summer) and rabi (winter). Rice, cotton, and kharif fodder (maize and sorghum) are grown in kharif season, whereas wheat and rabi fodder (mostly barseem) are grown in rabi season [51]. Sugarcane is an annual crop, which is mostly cultivated in February and September as well. Figure 2 represents the crop calendar of main crops grown in Multan division.

## 2.2 Image classification

Landsat images of Landsat 4, 5 Thematic Mapper (TM), Landsat 7 Enhanced TM Plus (ETM+), and Landsat 8 OLI were used for the analysis of cropping pattern and LST

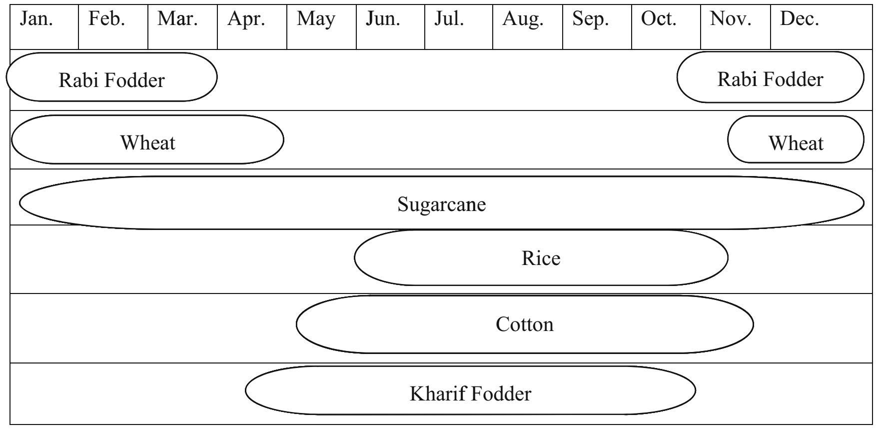


**Figure 2:** Cropping calendar adopted in the Southern Punjab. Rabi expresses the winter crop and kharif expresses the summer crop.

changes (Table 1). For this research, Landsat images were downloaded for 4 years (1990, 2000, 2010, and 2020) from official national aeronautics and space administration (NASA) Earth Explorer United States Geological Survey website (earthexplorer.usgs.gov).

Landsat images were preprocessed for georeferencing, layer stacking, and mosaicking by using GIS software: Arc GIS 10.4 and ERDAS imagine 15 [42]. Process of sub setting was used by using Arc GIS 10.4 software based on the study area [43,44]. Landsat images were then processed through supervised classification with digital topographic map of the Multan division. For our research, LULC classification was achieved with 0.97 convergence threshold and 50% iterations [45]. To assist Iterative Self Organizing Data Analysis Technique (ISODATA) algorithm, more refining of results was done by seeking farmers' opinion considering various cropping patterns in Multan division. Using ISODATA clustering process at 30 m × 30 m spatial resolution, LULC classes were treated separately for both kharif and rabi cropping seasons. The comparative benefit is that this classification is appropriate for forestry, water resources, and agricultural studies. Furthermore, spectral signature of cultivated area for separate fodder did not exist from other source to confirm greatest accuracy of postclassification. Bare soil and built-up area were combined to one class (built-up/barren); therefore, five LULC classes were defined for rabi seasons including sugarcane, wheat, water bodies, built-up/barren, and rabbi fodder (barseem and vegetables), and six classes were defined for kharif season comprising sugarcane, cotton, rice, water bodies, built-up/barren, and kharif fodder (sorghum, maize, and vegetables, etc.) in the study area.

A survey of 420 farms was undertaken to collect information about crop information and LULC changes. A total of 35 union councils were selected from each district; from every union council, three villages were selected by simple random method. GPS Essential software was used to attain the latitude and longitude points. It is smartphone-based application, which permits collecting the georeferenced and digital field information. Areal distribution for all LULC classes was calculated for both cropping seasons from 1990 to 2020 over the whole study period. The relationship of temperature with NDVI for each cropping season was drawn. The details of methodology are given in Figure 3.

**Table 1:** Specification of Landsat satellite images

| No. | Satellite/sensor | Pixel size | Spectral resolution | Band used | Path/row | Date |
|---|---|---|---|---|---|---|
| 1 | LANDSAT 5 | 30 m | Multispectral (8 bands) | 1–5,7 | 150/039 | March, 1990 |
| | | | | | 150/040 | September, 1990 |
| 2 | LANDSAT 5 | 30 m | Multispectral (8 bands) | 1–5,7 | 149/039 | March, 2000 |
| | | | | | 149/040 | September, 2000 |
| 3 | LANDSAT 7 | 30 m | Multispectral (11 bands) | 1–7,9 | 150/039 | March, 2010 |
| | | | | | 150/040 | September, 2010 |
| 4 | LANDSAT 8 | 30 m | Multispectral (11 bands) | 1–7,9 | 150/039 | March, 2020 |
| | | | | | 150/040 | September, 2020 |

## 2.3 Estimation of NDVI

Different Landsat images were used for the analysis of NDVI changes (Table 1). The NDVI was computed as follows [47,48]:

$$\mathrm{NDVI} = \frac{\mathrm{NIR} - \mathrm{RED}}{\mathrm{NIR} + \mathrm{RED}}, \tag{1}$$

where NIR is near-infrared band (TM and ETM + band 4, OLI band 5), and RED is the red band (TM and ETM + band 3, OLI band 4). NDVI value ranges between –1 and +1.

Vegetation indices such as NDVI (time-based) profiles were used to combine various classes as well as to identify crop growth phases like sowing and harvesting [46]. The NDVI were derived for the mentioned study period (30 years) for Multan region. Such NDVI images were reclassified by using software Arc GIS 10.4 to compare the changes found in the study duration.

## 2.4 Classification accuracy assessment

Error matrix is a quite general widespread means to show accuracy outcomes. Different statistical processes of thematic accuracy can be drawn from the error matrix; for example, percentage of user's accuracy, producer's accuracy, and overall accuracy address the error produced by chance [49,50].

$$\text{Overall accuracy} = \frac{N_{\mathrm{sc}}}{N_{\mathrm{rc}}}, \tag{2}$$

In equation (2), $N_{\mathrm{sc}}$ is the number of sampling classes classified correctly, and $N_{\mathrm{rc}}$ is the number of reference sampling classes. The KHAT ($\hat{k}$) values are an estimate of how well RS classification is correct and agree with reference data conceptually, $\hat{k}$ can be defined as follows [51]:

$$\hat{k} = \frac{A_{\mathrm{o}} - C_{\mathrm{a}}}{1 - C_{\mathrm{ag}}}, \tag{3}$$

In equation (3), $A_{\mathrm{o}}$ is the observed accuracy, $C_{\mathrm{a}}$ is the chance assessment, and $C_{\mathrm{ag}}$ is the chance agreement. This statistic serves as an indicator of the extent to which the percentage correct values of an error matrix are due to "true" vs "chance" agreement.

## 2.5 Estimation of LST

LST is a general term relating to combined temperature of intact objects existing on the land. Numerous researchers used defined measurement on Landsat images to

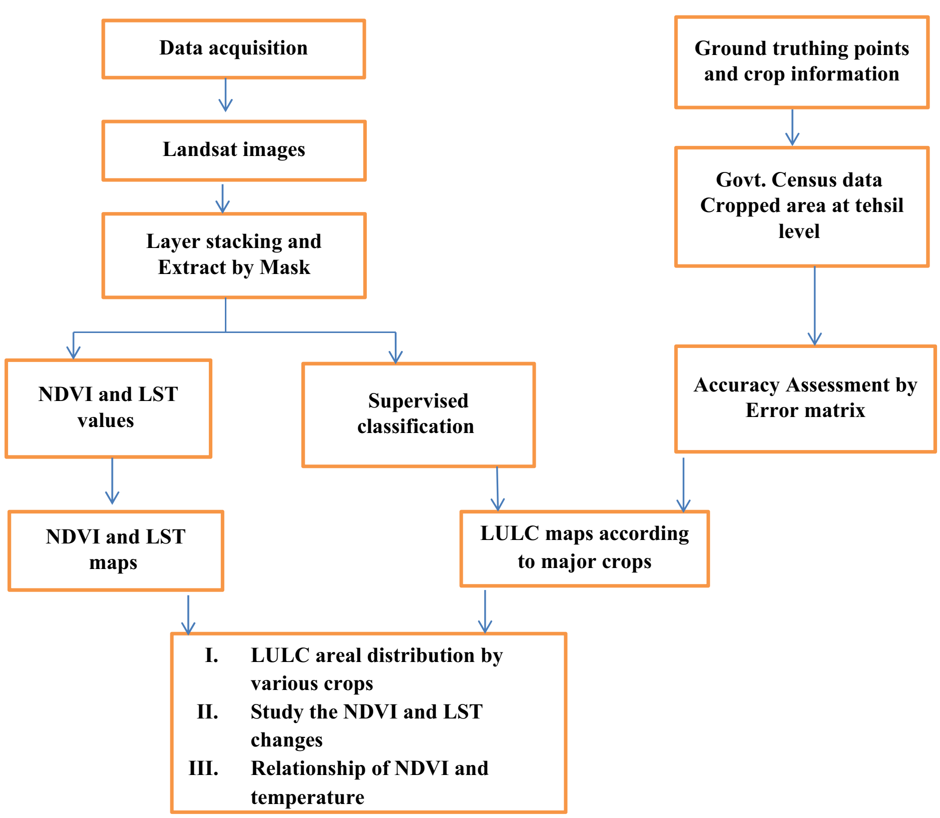


**Figure 3:** Flow diagram showing methodological and analytical steps.

estimate the LST [52]. The LST was estimated from the OLI Landsat 8 thermal infrared band (band 10) with spatial resolutions of 30 m, respectively [53]. First, $L\lambda$ values were estimated to spectral radiance by equation (4) [54].

$$L\lambda = \text{gain} \times \text{QCAL} + \text{offset}, \tag{4}$$

$L\lambda$ denotes spectral radiance and QCAL is quantized calibrated pixel value in digital number.

In the second step, the spectral radiance value was converted to temperature by using equation (5) [55].

$$T = \frac{K_2}{\ln\left(\frac{K_1}{L\lambda} + 1\right)}, \tag{5}$$

where $K_1$ and $K_2$ values are 607.76 and 1260.56 for Landsat 4/5 (TM) and Landsat 7 (ETM+), and 772.88 and 1321.07 for Landsat 8 (OLI), respectively, and ln shows natural logarithm. In the last step, temperature in Kelvin (K) was converted to Celsius (°C) through equation (6) [56].

$$T(°\text{C}) = T(\text{K}) - 273.15. \tag{6}$$

# 3 Results and discussion

## 3.1 Areal distribution of major crops

Assessment of areal distribution for different LULC classes forms vital information for hydrological modeling mainly in watershed agriculture. The maps of LULC were obtained to identify the various crops in kharif and rabi seasons in Multan region. Figure 4 indicated the dominance of arable vegetation area in Multan division. Wheat and cotton were dominated crops during rabi and kharif periods, respectively. Rice was dominated in the downstream region along with sugarcane. For rabi seasons, a characteristic pattern in crop-cultivated land was perceived at different intervals in the study area. The cultivation of wheat showed most relative variation in area, that is, 1165106.73 ha (65.27%) and 1070775.22 ha (59.98%) in 1990 and 2020, respectively. Wheat area was decreased 5.28% during 1990–2020 in Multan region (Table 2). Minimum and maximum areas of sugarcane were 273827.24 ha (15.34% during 1990) and 221766.66 ha (12.42% during 2020), respectively. The cultivated area under sugarcane decreased 2.92% from 1990 to 2020. Minimum and maximum areas for rabi fodder (like barseem and vegetables etc.) were observed 10.4% during 1990 and 15.72% during 2020, respectively, whereas built-up/barren area were 7.03% during 1990 and 10.53% during 2020 (Figure 4). Build-up area increased 3.5% during 1990–2020 in Multan region. The water bodies showed relative variation in area, that is, 35054.01 ha (1.96%) and 23919.65 ha (1.34%) in 1990 and 2020, respectively, which decreased by 0.62% during 1990–2020. The decrease in water resources has also been one of the main reasons in the reduction of rice and sugarcane area in Multan region. It is worth observed that during the last 30 years, almost the (8%) wheat and sugarcane area transformed to fodder, cash crop maize, and other valuable vegetable crops as well as built-up area.

During all kharif seasons, cotton was the main class in Multan division with a total cropped land ranging between 625973.33 ha (35.01% in 1990) and 508358.75 ha (28.48% in 2020). Cotton area decreased 6.59% during 1990–2020 in the study area. Rest of the area was under cultivation of sugarcane and rice with values ranging 15.54–12.65% for sugarcane and 21.57–19.96% for rice during the study period (Table 3). Minimum and maximum areas for kharif fodder (like maize, vegetables, etc.) were observed in 1990 (17.85%) and in 2020 (26.34%), respectively. The built-up area increased from 7.31 to 10.95% during 1990–2020. The shortfall in production is attributed to the decline in cotton area sown due to water shortage, cotton leaf curl virus, and high prices of synthetic spray of insecticides and pesticides. The cultivation and production of the maize crop increased due to the increase in area sown and as good economic returns and comparatively timely payment encouraged the growers to bring more area under maize cultivation. According to an earlier study [34], cropping pattern of different crops has changed and LST has increased during the last few years in the Multan district.

## 3.2 Accuracy assessment

Accuracy assessment in Table 4 shows the year wise detail of producer and user accuracies for various LULC classes including the kharif and rabi crops, water bodies, and barren land/buildings. The average of producer accuracy for kharif crops of cotton, rice, sugarcane, and fodder were 84.7, 84.2, 83.6, and 82.0%, respectively. Similarly, the average user accuracy for the four crop classes were 80.9, 80.9, 84.1, and 80.4% in the respective order. Similarly, the producer and user accuracies for rabi crops wheat, sugarcane, and fodder were 89.1 and 87.7, 80.3 and 80.0, and 78.6 and 81.3%, respectively.

In Table 5, we see year wise trend of overall accuracy and $K$ values in addition to producer and user accuracies. The maximum overall accuracy of kharif season (84.8%) and rabi season (87.2%) were obtained in 1990, whereas the highest $K$ value of kharif (85%) and rabi (87%) were obtained in 2000 and 2010, respectively. In Table 6, a brief overview of overall accuracy and $K$ values of

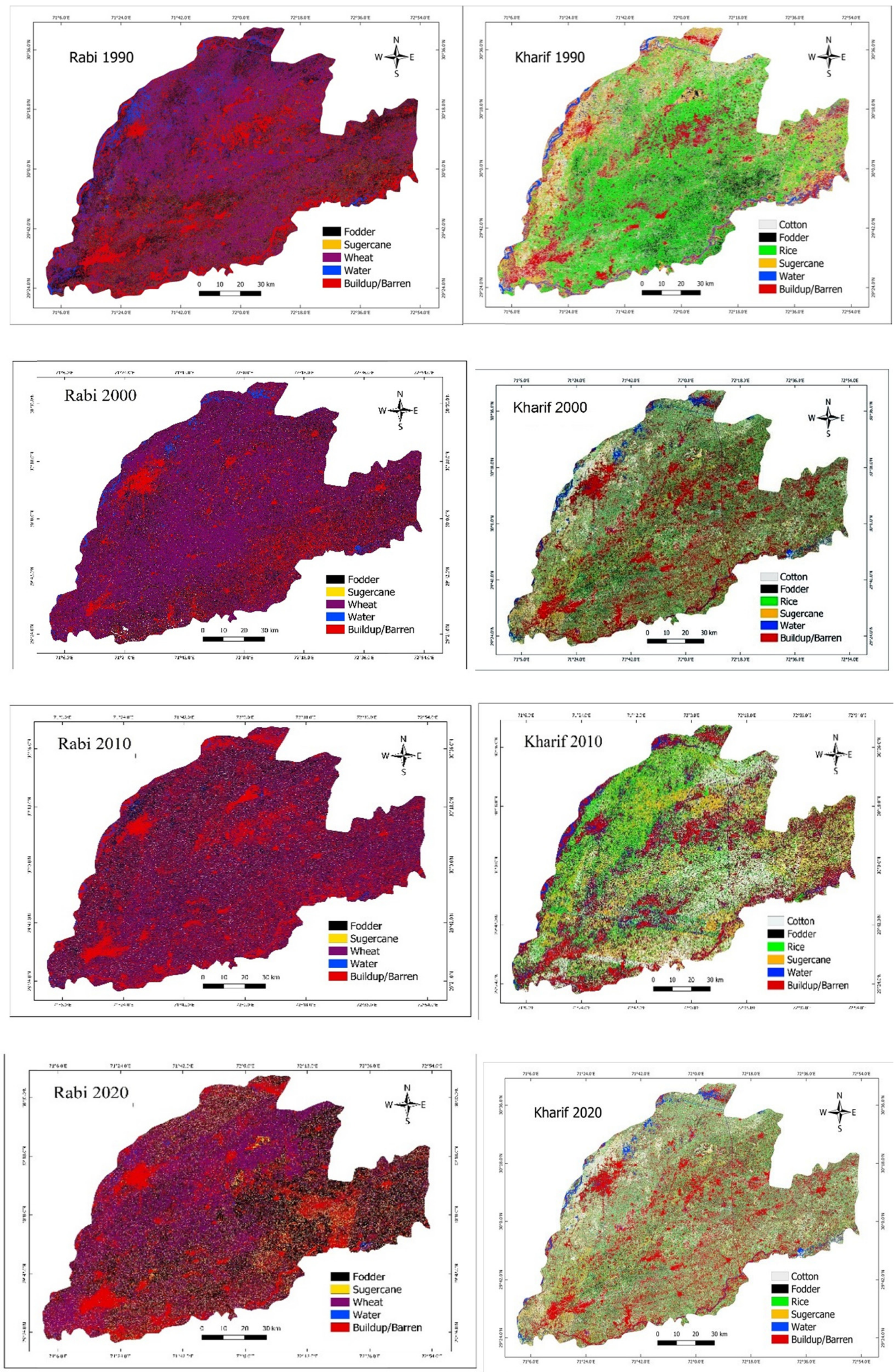


**Figure 4:** Crop identification maps for rabi and kharif seasons from 1990 to 2020.

**Table 2:** Areal distribution of different LULC classes in rabi seasons in Multan division

| No. | LULC classes | 1990 | | 2000 | | 2010 | | 2020 | | Change from 1990 to 2020 | |
|---|---|---|---|---|---|---|---|---|---|---|---|
| | | ha | % | ha | % | ha | % | ha | % | ha | % |
| 1 | Rabi fodder | 185655.16 | 10.4 | 226250.07 | 12.67 | 246264.04 | 13.79 | 280675 | 15.72 | 95019.84 | 5.32 |
| 2 | Sugarcane | 273827.24 | 15.34 | 260534.26 | 14.59 | 246520.3 | 13.81 | 221766.66 | 12.42 | −52060.6 | −2.92 |
| 3 | Wheat | 1165106.73 | 65.27 | 1153570.55 | 64.62 | 1128586.53 | 63.22 | 1070775.22 | 59.98 | −94331.5 | −5.28 |
| 4 | Water bodies | 35054.01 | 1.96 | 30039.24 | 1.68 | 29039.25 | 1.63 | 23919.65 | 1.34 | −11134.4 | −0.62 |
| 5 | Build-up/barren | 125443.05 | 7.03 | 114692.07 | 6.44 | 134676.07 | 7.55 | 187949.66 | 10.53 | 62506.61 | 3.5 |
| | | 1785086.19 | 100 | 1785086.19 | 100 | 1785086.19 | 100 | 1785086.19 | 100 | | |

**Table 3:** Areal distribution of different LULC classes in kharif seasons in Multan division

| No. | LULC classes | 1990 | | 2000 | | 2010 | | 2020 | | Change from 1990 to 2020 | |
|---|---|---|---|---|---|---|---|---|---|---|---|
| | | ha | % | ha | % | ha | % | ha | % | ha | % |
| 1 | Cotton | 625973.33 | 35.01 | 623287.54 | 34.92 | 591124.04 | 33.11 | 508358.75 | 28.48 | −117615 | −6.59 |
| 2 | Kharif fodder | 318615.6 | 17.85 | 361238.36 | 20.24 | 383284.58 | 21.47 | 470177.37 | 26.34 | 151561.8 | 8.5 |
| 3 | Rice | 385143.55 | 21.57 | 372090.71 | 20.84 | 377261.5 | 21.13 | 356249.32 | 19.96 | −28894.2 | −1.62 |
| 4 | Sugarcane | 277397.19 | 15.54 | 264450.96 | 14.81 | 249671.18 | 13.99 | 225785.24 | 12.65 | −51612 | −2.89 |
| 5 | Water bodies | 47417.05 | 2.66 | 39532.07 | 2.21 | 37399.23 | 2.09 | 29058.81 | 1.63 | −18358.2 | −1.03 |
| 6 | Build-up/barren | 130539.47 | 7.31 | 124486.55 | 6.97 | 146345.66 | 8.2 | 195456.7 | 10.95 | 64917.23 | 3.64 |
| | | 1785086.19 | 100 | 1785086.19 | 100 | 1785086.19 | 100 | 1785086.19 | 100 | | |

previously conducted studies (based on the use of different satellites and their sensor) is given. This is a sort of comparison and it is clear that Landsat had better values (58, 59, 60, 50, and 34) than MODIS. The current study had also reasonable overall accuracy (82.5–84.1%) and $K$ value (80.0–81.5%). These values are compatible with already conducted studies and it shows the reliability of our results. The lower accuracy values in this comparison stem due to minor plot and combination of pixels sizes due to mixed cropping pattern during kharif season [57].

## 3.3 Cropping pattern and NDVI

Two depressions and two peaks in one cropping year were detected in Multan division. The two depressions

**Table 4:** Producer's accuracy and user's accuracy for various classes

| LULC classes | | Crop seasons and classes | | | | | | | | | |
|---|---|---|---|---|---|---|---|---|---|---|---|
| | | Producers accuracy | | | | | Users accuracy | | | | |
| | | 1990 | 2000 | 2010 | 2020 | Avg. | 1990 | 2000 | 2010 | 2020 | Avg. |
| Kharif | 1 | 88.2 | 82.5 | 85.7 | 82.5 | 84.7 | 78.2 | 81.2 | 78.2 | 85.9 | 80.9 |
| | 2 | 84.4 | 79.3 | 83 | 90.2 | 84.2 | 79.2 | 84.3 | 81.5 | 78.6 | 80.9 |
| | 3 | 84.7 | 82.4 | 82.5 | 84.6 | 83.5 | 83 | 86.1 | 82.2 | 85.2 | 84.1 |
| | 4 | 76.9 | 83.1 | 85.2 | 82.9 | 82.02 | 83.7 | 80.3 | 77.8 | 79.7 | 80.4 |
| | 5 | 78.1 | 87.5 | 87.5 | 85.8 | 84.72 | 77.5 | 73.9 | 78.7 | 82.8 | 78.2 |
| | 6 | 82.2 | 84 | 87 | 92 | 86.4 | 81.5 | 78.2 | 81.9 | 83 | 81.1 |
| Rabi | 7 | 90 | 87.1 | 93.3 | 85.9 | 89.1 | 87.1 | 88.7 | 90.6 | 84.5 | 87.7 |
| | 8 | 82.8 | 72.9 | 80.2 | 85.5 | 80.3 | 72.8 | 81 | 85.2 | 80.9 | 80 |
| | 9 | 78.3 | 76.7 | 78.7 | 80.6 | 78.6 | 85.2 | 76.3 | 85.8 | 77.8 | 81.3 |
| | 10 | 79.4 | 81.5 | 80.4 | 84.8 | 81.5 | 82.9 | 80.4 | 85 | 84.3 | 83.1 |
| | 11 | 82.6 | 79.5 | 83.1 | 84 | 82.3 | 82 | 81.5 | 86.6 | 81.9 | 83 |

Where for Kharif: 1, cotton; 2, rice; 3, sugarcane; 4, Kharif fodder; 5, water bodies; and 6, built-up/barren and for Rabi: 7, wheat; 8, sugarcane; 9, rabi fodder; 10, water bodies; and 11, built-up/barren.

**Table 5:** Detail of periodic kappa coefficients and accuracies

| Sr. No. | Year | Kharif seasons | | | | Rabi seasons | | | |
|---|---|---|---|---|---|---|---|---|---|
| | | Avg. prod. accuracy | Avg. user accuracy | Overall accuracy | *K* | Avg. prod. accuracy | Avg. user accuracy | Overall accuracy | *K* |
| 1 | 1990 | 82.5 | 80.5 | 84.8 | 79 | 82.6 | 82 | 87.2 | 82 |
| 2 | 2000 | 83.1 | 80.6 | 82.5 | 85 | 79.5 | 81.6 | 81.5 | 79 |
| 3 | 2010 | 85.1 | 80 | 79 | 82 | 83.1 | 86.6 | 85 | 87 |
| 4 | 2020 | 88.28 | 82.5 | 83.7 | 80 | 84. | 81.9 | 82.9 | 72 |
| Average | | 83.7 | 80.9 | 82.5 | 81.5 | 82.4 | 83.0 | 84.1 | 80 |

**Table 6:** Comparison of *K* values and accuracy values from previous studies with the current study

| Sr. No. | References | Type of data | Overall accuracy | *K* |
|---|---|---|---|---|
| 1 | [58] | Landsat MSS. ETM+ | 84.4–87.1 | 82.3–83.6 |
| 2 | [59] | Landsat | 78–92 | 84–93 |
| 3 | [51] | MODIS | 78.2–82.8 | 71–73 |
| 4 | [60] | Landsat | 87–91 | 84–90 |
| 5 | [50] | Landsat | 86.7–93.6 | 84–94 |
| 6 | [34] | Landsat | 85.7–87.7 | 78–81 |
| 7 | Present study | Landsat | 82.5–84.1 | 80–81.5 |

seemed at end of month of April (on harvesting of wheat) and earlier in month of November (before sowing of wheat). The first peak corresponded to the extreme growth of wheat in February to March. The second peak corresponding to cotton at its extreme growth was observed during August to September. Sowing of wheat started at the end of November in the study area; however, an NDVI value became greatest during the month of February (Figure 5). The class "rice" in kharif period had a unique tendency. The early part was lengthy and bit slack because of growth of rice from June to July; whereas, the late part attained extreme height due to fast rice growth during the last week of August (Figure 5). Sugarcane was mostly cultivated during February. Its graph remained low and static in rabi season and reached to maximum values during kharif season due to increased vegetative growth. The class "building" showed the minimum NDVI values during the year due to less reflectance, which is according to earlier results by Cheema and Bastiaanssen [57]. Outcome of this satellite-based study showed that during 1990–2020 cropping seasons, various cropping patterns were executed by the local farmers in Multan division, namely "Rice–Wheat–Rice," "Cotton–Wheat–Cotton," "Wheat–Sugarcane–Wheat," and "Wheat–Maize–Wheat." This pattern of cropping was similar with the actual dominant system as shown during survey of the study area.

As regards NDVI, its values ranged in 1990 from −0.05 to +0.6; however, in 2000, NDVI showed the minimum value −0.09 and maximum +0.58 (as shown in Table 7). The NDVI values ranged from −0.12 to 0.55 in 2010 and from −0.15 to 0.54 in 2020 in the study area. This NDVI trend showed that average NDVI values decreased from 0.27 to 0.19 during 1990–2020 in the study area (Table 7). The NDVI is one of the commonly used indices to distinguish between healthy vegetation and vegetated regions from stressed and nonvegetated lands. The NDVI values identify the amount of chlorophyll content found in vegetation, wherever maximum NDVI value show dense and healthy vegetation and least NDVI value show bare soil and sparse vegetation. Therefore, as water absorbed electromagnetic radiations, water areas gave negative NDVI values. Similarly, Figure 6 is based on categorization of different land uses on the basis of NDVI in the month of March. It shows that vegetation was dense in most parts of the Multan region and the buildings occupied the less area in 1990 (as shown by green color having NDVI values >0.50). This situation transformed during subsequent years. We see that the vegetation area was occupied by more buildings in 2000, 2010, and 2020. In 2020, the highest number of buildings and/or barren land could be seen especially in Multan district (as shown by red color having NDVI <0). More towns have been constructed in the suburbs of cities where vegetation previously existed, or the vegetation area has been occupied by public and private property developers leaving the land barren at a vast area [58]. This situation could be alarming from agricultural point of view if no proper planning is executed to accommodate useless or less productive land for town development instead of productive area [60].

## 3.4 LST

The previous data of maximum and minimum temperatures for the 30 years (1990–2020) of Southern Punjab were

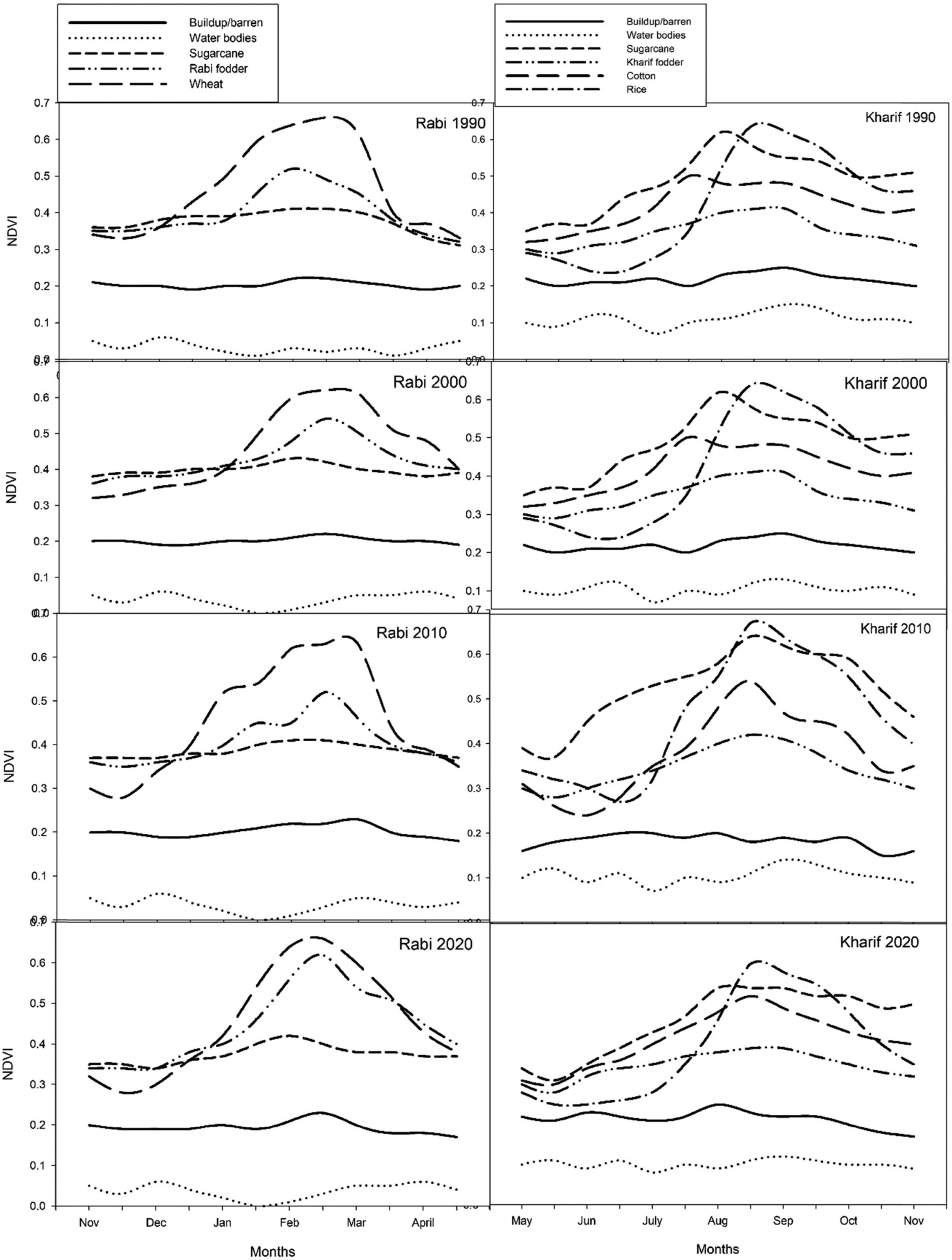


**Figure 5:** NDVI time-based tendencies for main crops from 1990 to 2020.

**Table 7:** Maximum and minimum values of NDVI and LST from 1990 to 2020

| Years | NDVI min | NDVI max | Average | LST min | LST max | Average |
|---|---|---|---|---|---|---|
| 1990 | −0.05 | 0.6 | 0.27 | 18.5 | 36.7 | 27.6 |
| 2000 | −0.09 | 0.58 | 0.24 | 19.6 | 36.2 | 27.9 |
| 2010 | −0.12 | 0.55 | 0.21 | 19 | 37.3 | 28.15 |
| 2020 | −0.15 | 0.54 | 0.19 | 19.2 | 37.8 | 28.5 |

attained from NASA website (http://power.larc.nasa.gov). Minimum temperature trend showed a slight decrease from 1990 to 1994, a trend reversed in 1996; considerable changes in the mean minimum temperature from 19 to 21°C were observed from 2014 onward. Maximum temperature trend during 1990–1995 showed a slight decrease, a similar trend as maximum temperature during 2014, an absolute increase in maximum temperature onward 2020 (Figure 7). The average temperature was observed 27.5°C (1990) and 28.6°C (2020), so an increase of 1.1°C in the average temperature was observed in Multan division during 1990–2020.

LST in Multan region for the month of March is shown in Figure 8. The results showed that LST values increased during 1990–2020, which was due to more built-up area producing maximum thermal signal. For the year 1990, LST ranges dominated in Multan region were from 18.5 to 36.7°C, and for the year 2000, LST

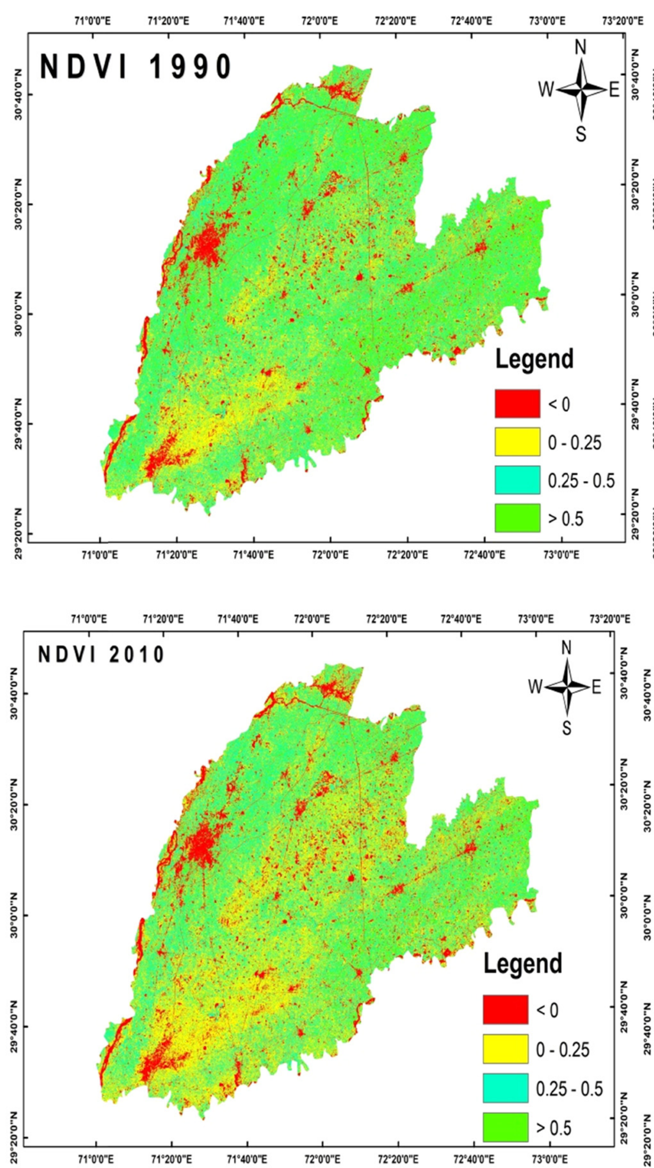


**Figure 6:** NDVI map of the study area during March for 1990–2020.

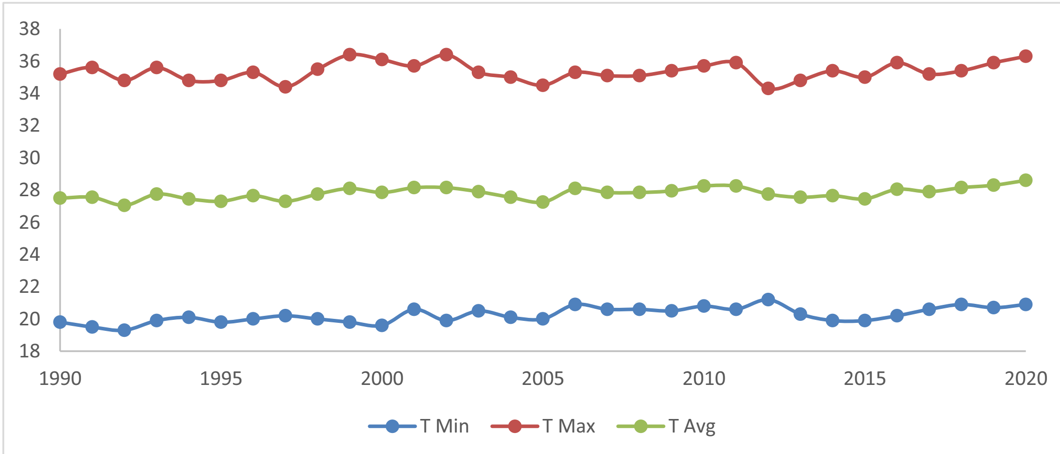


**Figure 7:** Average temperature trend of the study area from 1990 to 2020.

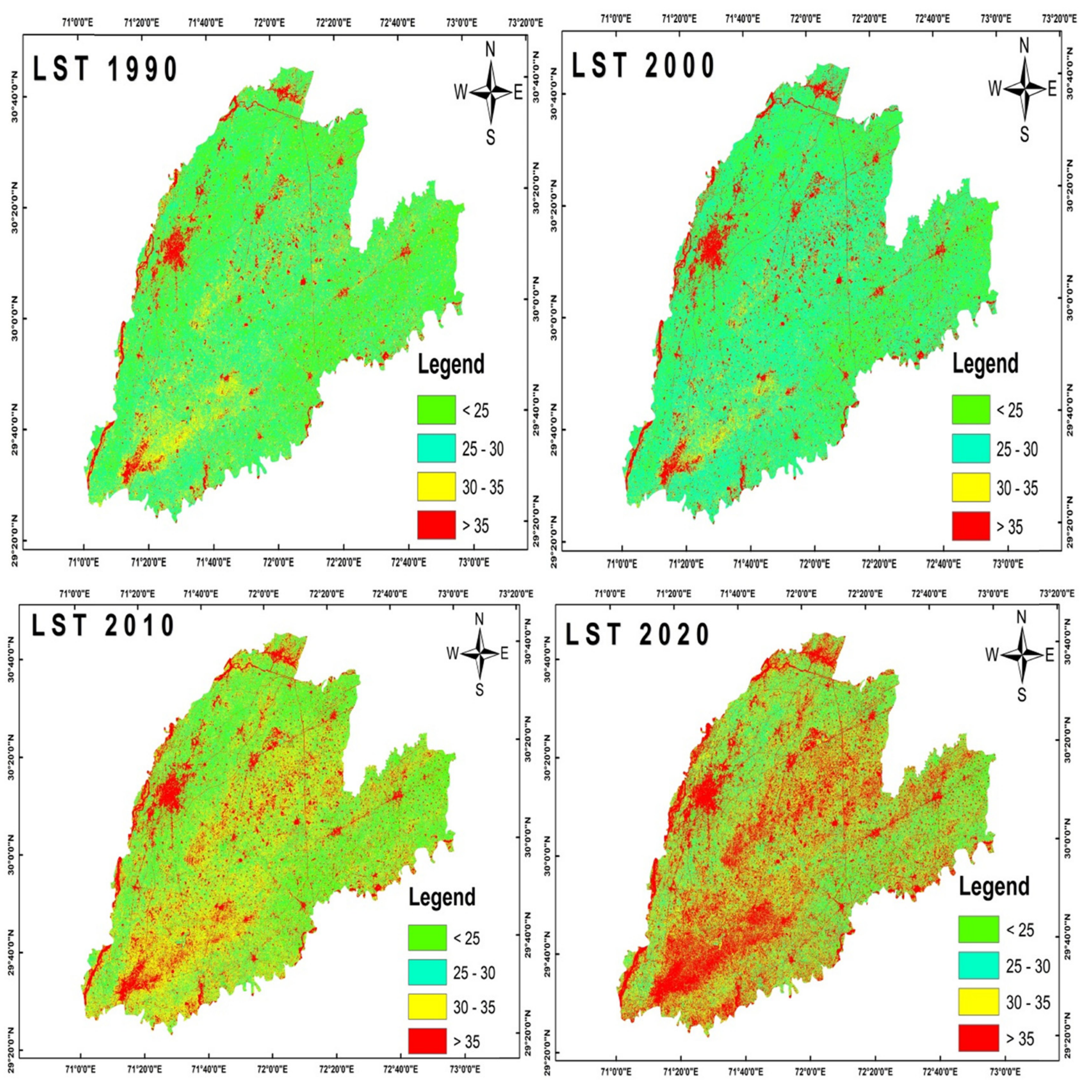


**Figure 8:** LST maps of the study area during 1990–2020.

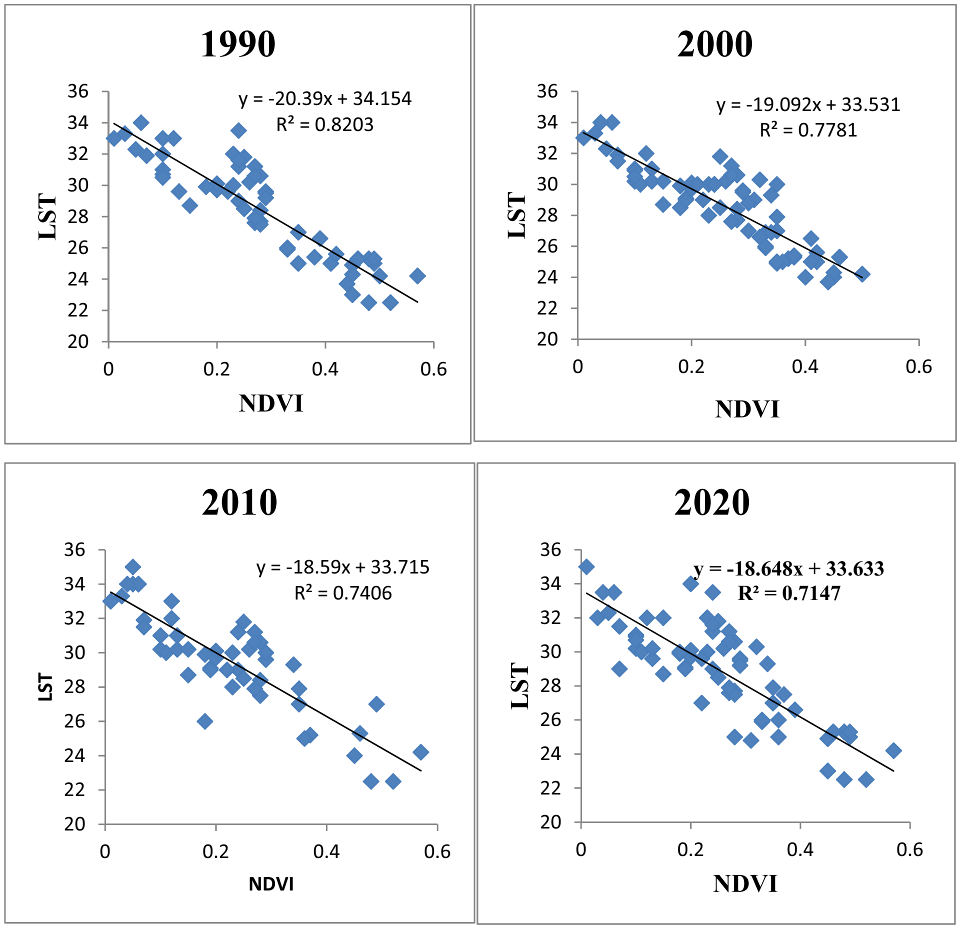


**Figure 9:** Regression analysis of NDVI and LST from 1990 to 2020.

ranged from 19.6 to 36.2°C in the study area. However, in 2010, LST values ranged from 19 to 37.3°C, and in year 2020, LST values ranged from 19.2 to 37.8°C (Table 7). In Multan region, high temperature was perceived in the built-up area because this area is more developed in terms of infrastructure than surrounding area. It is observed that the average LST values increased from 27.6 to 28.5°C during 1990–2020 due to increasing built-up area in Multan region. These facts are also supported by the comparison of Figure 6 with Figure 8, and we see that in southern part of Multan region, the infrastructural development and fallowing of cropping land for town purpose has not only led to the decrease in the value of NDVI but also resulted in more LST. It is most useful to have knowledge and information of LST to estimate and assess the urban surrounding climate. According to an earlier study [34], high temperature was observed in built-up area and bare soil because this area is more developed in terms of infrastructure than the surrounding area. Similarly, low temperature was recorded in vegetation area such as forest, wheat, rice, cotton, and sugarcane. This is more of true that in areas proximal to city buildings and roads in Multan region, the agricultural production is appreciably decreased due to increasing temperature and less rainfall; hence, the vegetation pattern has been changed and people have shifted from agronomic crops (wheat, cotton, etc.) to horticultural crops (vegetables, etc.) and fodder [61]. According to Amin et al. [62], uneven increase in precipitation and asymmetric increase in temperature extremes in the future would also increase the risk associated with management of climatic uncertainties. According to Amin et al. [63], southern Punjab has much agricultural production and has great contribution in total economic condition of the country; therefore, any temperature variations may affect the agriculture productivity.

## 3.5 Relationship of NDVI and LST

To identify and assess the relationship of NDVI and LST in the study area, regression analysis was used between NDVI and LST values from the survey points for the month of March; the regression $R^2$ analysis showed that LST and NDVI were negatively connected. In cropping seasons, nature of control ($R^2$ = 0.82, 0.77, 0.74, and 0.71) was observed in 1990, 2000, 2010, and 2020, respectively (Figure 9). Most of the cluster of NDVI values was found to be from −0.05 to +0.6 in 1990; however, it was shifted to −0.15 to +0.54 in 2020 (Table 7). The NDVI values for Multan region, was higher in 1990 to +0.6 and lowest in 2020 to −0.15. The LST values for Multan region, was higher in 2020 to 37.8°C and lowest in 1990 to 18.5°C. The LST depends on soil moisture, thermal characteristics and particle size of a soil, whereas NDVI trend depends on physio-chemical features of leaf and plant texture. Policy orientation, market, and other factors affect the change of agricultural planting structure and also affect the change of LULC. The change of LULC leads to the great change of underlying surface, and then affects the change of surface temperature. These results show that the vegetation-covered areas can also be decreased because of the surface temperature. The negative relationship between NDVI and LST identifies that the greater biomass of vegetation cover has lower LST [34]. It also implies that the territories showing the most reduced NDVI values have a less vegetal spread due to the urban extension, whereas the higher NDVI values have a thick vegetal spread, and in this way, LST increase with the abatement in the vegetal density [64]. Some studies show that intact land-covers slowed down the increase in the surface temperature for mid and high latitudes in the region of North America and Eurasia over a period of 20 years. But this finding may be effective for a narrow range of temperature increases. So, if the temperature increases too quickly, or if the temperature increase crosses some critical value, then the vegetation may decline. Statistical estimates are consistent with this potential and show that there is an inverted U-shaped relation between summer temperature and summer NDVI for most of the land covers in the region of Eurasia [65,66].

## 4 Conclusion

In this study, utilization of Landsat images identified the LULC changes for cropping seasons (like rabi season and kharif season) and their effect on LST for a 30 year time span (from 1990 to 2020 in Multan region). The error matrix analysis indicates overall accuracy changing from 82.5 and 84.1% during kharif and rabi season, respectively. Kappa values varied from 79 to 80% for kharif periods; however, these ranged 82–72% for rabi season. The NDVI values in 1990 were from −0.05 to +0.6; however, in 2020, NDVI indicated the least value both in minimum and maximum values, that is, −0.15 and +0.54. The average temperature increased from 27.6 to 28.5°C in the Multan region between 1990 and 2020. This temperature increase in the study area was slightly higher than the background global warming and climate change. Increasing comforts have the harmful impact on LST, which is increasing at a fast pace in Multan region. Our outcome also showed that the increasing temperature in growing season had an overriding impact on vegetation dynamics including major crops in Multan division. The LULC changes show that sugarcane and rice (decreasing by 2.9 and 1.6%, respectively) had less volatility of variation in comparison with both wheat and cotton (decreasing by 5.3 and 6.6%, respectively). The response of various vegetation types to environment variability also changed significantly. These variations caused an increase in LULC changes and LST values. Climate change including LST has an impact on various crops, such as growth conditions for cotton and rice crops much changed in Multan region. Hence, a crop-based classification aids water policy managers and analysts to make a better policy with enhanced information based on the extent of the natural resources. In future, this study should be useful for studying various crops using other satellites such as Sentinel and in the platform of Google earth engine. This study could form the basis of estimating the crop yields using satellite tools in various regions.

**Acknowledgements:** The authors are thankful to the COMSATS University Islamabad for financial support under COMSATS Research Grant Program (CRGP).

**Authors contribution:** Experimental concept: SH, MM, HMH, MA, and MI; methodology: SH, MM, AA, and MU; software: SH, MM, MU, and MW; formal analysis: HUF, SF, and WN; original draft preparation, SH, MM, and HMRJ; and writing – review and editing, NM, MA, SAQ, AF, and SK. All authors have read and agreed to the published version of the manuscript. The authors applied the SDC approach for the sequence of authors. In this case, SDC means that the sequence of authors reflects the declining importance of their contribution.

**Conflict of interest:** Authors state no conflict of interest.

## References

[1] Akram R, Turan V, Hammad HM, Ahmad S, Hussain S, Hasnain A, et al. Fate of organic and inorganic pollutants in paddy soils. Environmental Pollution of Paddy Soils. Cham:

Springer; 2018. p. 197–214. doi: 10.1007/978-3-319-93671-0_13.
[2] Zahoor SA, Ahmad S, Ahmad A, Wajid A, Khaliq T, Mubeen M, et al. Improving water use efficiency in agronomic crop production. Agronomic Crop. Singapore: Springer; 2019. p. 13–29. doi: 10.1007/978-981-32-9783-8_2.
[3] Mubeen M, Bano A, Ali B, Islam ZU, Ahmad A, Hussain S, et al. Effect of plant growth promoting bacteria and drought on spring maize (*Zea mays* L.). Pak J Bot. 2021;53(2):1–10. doi: 10.30848/PJB2021-2(38).
[4] Chaudhuri G, Mishra NB. Spatio-temporal dynamics of land cover and land surface temperature in Ganges-Brahmaputra delta: a comparative analysis between India and Bangladesh. Appl Geo. 2016;68:68–83. doi: 10.1016/j.apgeog.2016.01.002.
[5] Rahman MTU, Tabassum F, Rasheduzzaman M, Saba H, Sarkar L, Ferdous J, et al. Temporal dynamics of land use/land cover change and its prediction using CA-ANN model for southwestern coastal Bangladesh. Env Monit Assess. 2017;189(11):565. doi: 10.1007/s10661-017-6272-0.
[6] Hussain S, Ahmad A, Wajid A, Khaliq T, Hussain N, Mubeen M, et al. Irrigation scheduling for cotton cultivation. Cotton Production and Uses. Singapore: Springer; 2020a. p. 59–80. doi: 10.1007/978-981-15-1472-2_5.
[7] Policelli F, Hubbard A, Jung H, Zaitchik B, Ichoku C. Lake chad total surface water area as derived from land surface temperature and radar remote sensing data. Remote Sens. 2018;10(2):252. doi: 10.3390/rs10020252.
[8] Hussain S. Land use/land cover classification by using satellite NDVI tool for sustainable water and climate change in Southern Punjab. COMSATS University Islamabad; 2018, MS thesis, Pakistan. doi: 10.13140/RG.2.2.32363.69923.
[9] Nagendra H, Nagendran S, Paul S, Pareeth S. Graying, greening and fragmentation in the rapidly expanding Indian city of Bangalore. Landsc Urban Plan. 2012;105(4):400–6.
[10] Ayele GT, Tebeje AK, Demissie SS, Belete MA, Jemberrie MA, Teshome WM, et al. Time series land cover mapping and change detection analysis using geographic information system and remote sensing, northern Ethiopia. Air Soil Water Res. 2018;11:1178622117751603. doi: 10.1177/1178622117751603.
[11] Nayak DP, Fulekar MH. Coastal geomorphological and land use and land cover study on some sites of Gulf of Kachchh, Gujarat, West Coast of India using multi-temporal remote sensing data. Inter J Adv Remote Sens GIS. 2017;6(1):2192–2203. doi: 10.23953/cloud.ijarsg.273.
[12] Xiao X, Boles S, Frolking S, Li C, Babu JY, Salas W, et al. Mapping paddy rice agriculture in South and Southeast Asia using multi-temporal MODIS images. Remote Sens Env. 2006;100(1):95–113. doi: 10.1016/j.rse.2005.10.004.
[13] Chew C, Shah R, Zuffada C, Hajj G, Masters D, Mannucci AJ. Demonstrating soil moisture remote sensing with observations from the UK TechDemoSat-1 satellite mission. Geophy Res Lett. 2016;43(7):3317–24. doi: 10.1002/2016GL068189.
[14] Bento V, Trigo I, Gouveia C, DaCamara C. Contribution of land surface temperature (TCI) to vegetation health index: a comparative study using clear sky and all-weather climate data records. Remote Sens. 2018;10(9):1324. doi: 10.3390/rs10091324.
[15] Adeola AM, Olwoch JM, Botai JO, Rautenbach CD, Kalumba AM, Tsela PL, et al. Landsat satellite derived environmental metric for mapping mosquitoes breeding habitats in the Nkomazi municipality, Mpumalanga Province, South Africa. South Afr Geo J. 2017;99(1):14–28.
[16] Salari M, Shariat SM, Rahimi R, Dashti S. Land capability evaluation for identifying industrial zones: combination multi-criteria decision-making method with geographic information system. Int J Env Sci Technol. 2019;16:5501–12. doi: 10.1007/s13762-018-1925-2.
[17] Ding H, Shi W. Land-use/land-cover change and its influence on surface temperature: a case study in Beijing City. Inter J Remote Sens. 2013;34(15):5503–17. doi: 10.1080/01431161.2013.792966.
[18] Cai M, Ren C, Xu Y, Lau KKL, Wang R. Investigating the relationship between local climate zone and land surface temperature using an improved WUDAPT methodology – a case study of Yangtze River Delta, China. Urban Clim. 2018;24:485–502. doi: 10.1016/j.uclim.2017.05.010.
[19] Feizizadeh B, Blaschke T, Nazmfar H, Akbari E, Kohbanani HR. Monitoring land surface temperature relationship to land use/land cover from satellite imagery in Maraqeh County. Iran J Env Plan Manage. 2013;56(9):1290–1315.
[20] Zhang H, Qi ZF, Ye XY, Cai YB, Ma WC, Chen MN. Analysis of land use/land cover change, population shift, and their effects on spatiotemporal patterns of urban heat islands in metropolitan Shanghai, China. Appl Geo. 2013;44:121–33.
[21] Rozenstein O, Qin Z, Derimian Y, Karnieli A. Derivation of land surface temperature for Landsat-8 TIRS using a split window algorithm. Sens. 2014;14(4):5768–80.
[22] Ranjan AK, Anand A, Kumar PBS, Verma SK, Murmu L. Prediction of land surface temperature within sun city Jodhpur (Rajasthan) in India using integration of artificial neural network and geoinformatics technology. Asian J Geoinfo. 2018;17(3):1–12.
[23] Ige SO, Ajayi VO, Adeyeri OE, Oyekan KSA. Assessing remotely sensed temperature humidity index as human comfort indicator relative to landuse landcover change in Abuja. Niger Spat Info Res. 2017;25(4):523–33.
[24] Li L, Tan Y, Ying S, Yu Z, Li Z, Lan H. Impact of land cover and population density on land surface temperature: case study in Wuhan, China. J Appl Remote Sens. 2014;8(1):084993–9. doi: 10.1117/1.JRS.8.084993.
[25] Li X, Zhou W, Ouyang Z, Xu W, Zheng H. Spatial pattern of greenspace affects land surface temperature: evidence from the heavily urbanized Beijing metropolitan area. China Landsc Ecol. 2012;27(6):887–98.
[26] Aboelnour M, Engel BA. Application of remote sensing techniques and geographic information systems to analyze land surface temperature in response to land use/land cover change in greater Cairo region, Egypt. J Geo Info Sys. 2018;10(1):57–88. doi: 10.4236/jgis.2018.101003.
[27] Sayão VM, Demattê JA, Bedin LG, Nanni MR, Rizzo R. Satellite land surface temperature and reflectance related with soil attributes. Geoderma. 2018;325:125–40. doi: 10.1016/j.geoderma.2018.03.026.
[28] Bhagyanagar R, Kawal BM, Dwarakish GS, Surathkal S. Land use/land cover change and urban expansion during 1983-2008 in the coastal area of Dakshina Kannada district, South

India. J Appl Remote Sens. 2012;6(1):063576–9. doi: 10.1117/1.JRS.6.063576.
[29] Romaguera M, Vaughan RG, Ettema J, Izquierdo-Verdiguier E, Hecker CA, van der Meer FD. Detecting geothermal anomalies and evaluating LST geothermal component by combining thermal remote sensing time series and land surface model data. Remote Sens Env. 2018;204:534–52. doi: 10.1016/j.rse.2017.10.003.
[30] Liu YY, Parinussa RM, Dorigo WA, De Jeu RA, Wagner W, Van Dijk AIJM, et al. Developing an improved soil moisture dataset by blending passive and active microwave satellite-based retrievals. Hydro Earth Sys Sci. 2011;15(2):425–36. doi: 10.5194/hess-15-425-2011.
[31] Usman M, Liedl R, Shahid MA. Managing irrigation water by yield and water productivity assessment of a rice-wheat system using remote sensing. J Irrigat Drain Eng. 2014;140(7):04014022.
[32] Zoungrana B, Conrad C, Amekudzi L, Thiel M, Da E, Forkuor G, et al. Multi-temporal landsat images and ancillary data for land use/cover change (LULCC) detection in the Southwest of Burkina Faso, West Africa. Remote Sens. 2015;7(9):12076–102. doi: 10.1016/j.jaridenv.2018.01.005.
[33] Zoungrana BJ, Conrad C, Thiel M, Amekudzi LK, Da ED. MODIS NDVI trends and fractional land cover change for improved assessments of vegetation degradation in Burkina Faso, West Africa. J Arid Env. 2018;153:66–75. doi: 10.1016/j.jaridenv.2018.01.005.
[34] Hussain S, Mubeen M, Akram W, Ahmad A, Habib-ur-Rahman M, Ghaffar A, et al. Study of land cover/land use changes using RS and GIS: a case study of Multan district, Pakistan. Env Monit Assess. 2020b;192(1):2. doi: 10.1007/s10661-019-7959-1.
[35] Olmanson LG, Brezonik PL, Finlay JC, Bauer ME. Comparison of Landsat 8 and Landsat 7 for regional measurements of CDOM and water clarity in lakes. Remote Sens Env. 2016;185:119–28. doi: 10.1016/j.rse.2016.01.007.
[36] Ali M, Mubeen M, Hussain N, Wajid A, Farid HU, Awais M, et al. Role of ICT in Crop Management. Agronomic Crop. Singapore: Springer; 2019. p. 637–652. doi: 10.1007/978-981-32-9783-8_28.
[37] Onamuti OY, Okogbue EC, Orimoloye IR. Remote sensing appraisal of Lake Chad shrinkage connotes severe impacts on green economics and socio-economics of the catchment area. R Soc Open Sci. 2017;4(11):171120.
[38] Usman M, Liedl R, Awan UK. Spatio-temporal estimation of consumptive water use for assessment of irrigation system performance and management of water resources in irrigated Indus Basin. Pak J Hydro. 2015a;525:26–41.
[39] Sabagh AE, Hossain A, Islam MS, Iqbal MA, Fahad S, Ratnasekera D, et al. Consequences and mitigation strategies of heat stress for sustainability of soybean (Glycine max L. Merr.) production under the changing climate. Plant Stress Physiology. IntechOpen; 2020. doi: 10.5772/intechopen.92098.
[40] Ali A, Khalid A, Butt MA, Mehmood R, Mahmood SA, Sami J, et al. Towards a remote sensing and GIS-based technique to study population and urban growth: a case study of multan. Adv Remote Sens. 2018;7(03):245–58. doi: 10.4236/ars.2018.73017.
[41] Nasim W, Amin A, Fahad S, Awais M, Khan N, Mubeen M, et al. Future risk assessment by estimating historical heat wave trends with projected heat accumulation using SimCLIM climate model in Pakistan. Atmos Res. 2018;205:118–33. doi: 10.1016/j.atmosres.2018.01.009.
[42] Rani M, Kumar P, Pandey PC, Srivastava PK, Chaudhary BS, Tomar V, et al. Multi-temporal NDVI and surface temperature analysis for Urban Heat Island inbuilt surrounding of sub-humid region: a case study of two geographical regions. Remote Sens Applications: Soc Env. 2018;10:163–72. doi: 10.1016/j.rsase.2018.03.007.
[43] Kharazmi R, Tavili A, Rahdari MR, Chaban L, Panidi E, Rodrigo-Comino J. Monitoring and assessment of seasonal land cover changes using remote sensing: a 30 year (1987–2016) case study of Hamoun Wetland, Iran. Env Monit Assess. 2018;190(6):356. doi: 10.1007/s10661-018-6726-z.
[44] Shahzad H, Farid HU, Khan ZM, Anjum MN, Ahmad I, Chen X, et al. An integrated use of GIS, geostatistical and map overlay techniques for spatio-temporal variability analysis of groundwater quality and level in the Punjab Province of Pakistan, South Asia. Water. 2020;12(12):3555.
[45] Turk KG, Aljughaiman AS. Land use/land cover assessment as related to soil and irrigation water salinity over an oasis in arid environment. Open Geosci. 2020 Jul 6;12(1):220–31.
[46] Aredehey G, Mezgebu A, Girma A. Land-use land-cover classification analysis of Giba catchment using hyper temporal MODIS NDVI satellite images. Inter J Remote Sens. 2018;39(3):810–21. doi: 10.1080/01431161.2017.1392639.
[47] Tomar V, Kumar P, Rani M, Gupta G, Singh J. A satellite-based biodiversity dynamics capability in tropical forest. Electro J Geotech Eng. 2013;18(Bund. F):1171–80.
[48] Ahmad I, Saeed U, Fahad M, Ullah A, ur Rahman MH, Ahmad A, et al. Yield forecasting of spring maize using remote sensing and crop modeling in Faisalabad-Punjab Pakistan. J Indian Soc Remote Sens. 2018;46(10):1701–11. doi: 10.1007/s12524-018-0825-8.9.
[49] Hemba S, Iortyom ET, Ropo OI, Daniel DP. Analysis of the physical growth and expansion of Makurdi Town using remote sensing and GIS techniques. Imp J Interdiscip Res. 2017;3:821–7.
[50] Pal S, Ziaul SK. Detection of land use and land cover change and land surface temperature in English Bazar urban centre. Egypt J Remote Sens Space Sci. 2017;20(1):125–45.
[51] Usman M, Liedl R, Shahid MA, Abbas A. Land use/land cover classification and its change detection using multi-temporal MODIS NDVI data. J Geo Sci. 2015b;25(12):1479–1506. doi: 10.1007/s11442-015-1247-y.
[52] Liaqut A, Younes I, Sadaf R, Zafar H. Impact of urbanization growth on land surface temperature using remote sensing and GIS: a case study of Gujranwala City, Punjab, Pakistan. Inter J Eco Env Geo. 2019;9:44–9.
[53] Hussain S, Mubeen M, Ahmad A, Akram W, Hammad HM, Ali M, et al. Using GIS tools to detect the land use/land cover changes during forty years in Lodhran District of Pakistan. Env Sci Pollut Res. 2020c;27:39676–92. doi: 10.1007/s11356-019-06072-3.
[54] Sheela AM, Letha J, Joseph S, Ramachandran KK, Sanalkumar SP. Trophic state index of a lake system using IRS (P6-LISS III) satellite imagery. Env Monit Assess. 2011;177(1–4):575–92.
[55] Orimoloye IR, Mazinyo SP, Nel W, Kalumba AM. Spatiotemporal monitoring of land surface temperature and

estimated radiation using remote sensing: human health implications for East London, South Africa. Env Earth Sci. 2018;77(3):77. doi: 10.1007/s12665-018-7252-6.
[56] Forkel M, Carvalhais N, Verbesselt J, Mahecha M, Neigh C, Reichstein M. Trend change detection in NDVI time series: Effects of inter-annual variability and methodology. Remote Sens. 2013;5(5):2113–44. doi: 10.3390/rs5052113.
[57] Cheema MJM, Bastiaanssen WG. Land use and land cover classification in the irrigated Indus Basin using growth phenology information from satellite data to support water management analysis. Agri Water Manage. 2010;97(10):1541–52. doi: 10.1016/j.agwat.2010.05.009.
[58] Ahmad F. A review of remote sensing data change detection: comparison of Faisalabad and Multan Districts, Punjab Province, Pakistan. J Geo Reg Plan. 2012;5(9):236–51. doi: 10.5897/JGRP11.121.
[59] Reis S. Analyzing land use/land cover changes using remote sensing and GIS in Rize, North-East Turkey. Sens. 2008;8(10):6188–6202. doi: 10.3390/s8106188.
[60] Lu D, Li G, Moran E, Hetrick S. Spatiotemporal analysis of land-use and land-cover change in the Brazilian Amazon. Inter J Remote Sens. 2013;34(16):5953–78. doi: 10.1080/01431161.2013.802825.
[61] Hussain S, Karuppannan S. Land use/land cover changes and their impact on land surface temperature using remote sensing technique in district Khanewal, Punjab Pakistan. Geol Eco Landsc. 2021;1–13. doi: 10.1080/24749508.2021.1923272.
[62] Hussain S, Amin A, Mubeen M, Khaliq T, Shahid M, Hammad HM, et al. Climate smart agriculture (CSA) technologies. In: Jatoi WN, Mubeen M, Ahmad A, Cheema MA, Lin Z, Hashmi MZ, editors. Building climate resilience in Agr. Cham: Springer; 2022. p. 319–38. doi: 10.1007/978-3-030-79408-8_20.
[63] Amin A, Nasim W, Fahad S, Ali S, Ahmad S, Rasool A, et al. Evaluation and analysis of temperature for historical (1996-2015) and projected (2030-2060) climates in Pakistan using SimCLIM climate model: Ensemble application. Atmos Res. 2018b;213:422–36.
[64] Alqasemi AS, Ibrahim M, Fadhil Al-Quraishi AM, Saibi H, Al-Fugara A, Kaplan G. Detection and modeling of soil salinity variations in arid lands using remote sensing data. Open Geosci. 2021;13(1):pp. 443–53. doi: 10.1515/geo-2020-0244.
[65] Zhou L. Relation between interannual variations in satellite measures of vegetation greenness and climate between 1982 and 1999. J Geophys Res. 2003;108(D1):4004. doi: 10.1029/2002JD002510.
[66] Majeed M, Tariq A, Anwar MM, Khan AM, Arshad F, Shaukat S. Monitoring of land use–land cover change and potential causal factors of climate change in Jhelum district, Punjab, Pakistan, through GIS and multi-temporal satellite data. Land. 2021;10(10);1026. doi: 10.3390/land10101026.